Mathematical Modelling and Numerical Simulation with Applications, 2023, 3(1), 17–32

https://dergipark.org.tr/en/pub/mmnsa
ISSN Online: 2791-8564 / Open Access
https://doi.org/10.53391/mmnsa.1273945

RESEARCH PAPER

# Finite volume simulation of calcium distribution in a cholangiocyte cell

**Nakul Nakul** [1,‡], **Vedika Mishra** [1,*,‡] **and Neeru Adlakha** [1,‡]

[1]Department of Mathematics and Humanities, SVNIT, Surat, 395007, Gujarat, India

*Corresponding Author
‡i17ma040@amhd.svnit.ac.in (Nakul Nakul); d20ma001@amhd.svnit.ac.in (Vedika Mishra); nad@amhd.svnit.ac.in (Neeru Adlakha)

## Abstract

Cholangiocytes are the cells of the liver having a major role in the conditioning of bile used in digestion. Other functions of cholangiocytes are in apoptosis and bicarbonate secretion. The Calcium in the intracellular environment of various cells including cholangiocytes regulates a large number of functions. This regulating mechanism in cholangiocytes has been poorly understood to date. In order to analyze the calcium regulation in cholangiocyte cells, a mathematical model for a one-dimensional steady-state case is constructed in this study. This involves a non-linear reaction-diffusion equation with appropriate boundary conditions. The influx from $IP_3$ receptor, ryanodine receptor (RYR), and plasma membrane as well as the efflux of calcium from SERCA pump and plasma membrane have been employed in the model. The finite volume method and Newton-Raphson method have been used to solve the problem. Numerical findings have been used to examine the effects of parameters like diffusion coefficient, rate of SERCA pump efflux, buffer, and influx from plasma membrane on calcium concentration in cholangiocyte cells. The information generated from the model can be useful for understanding the mechanism of cholestatic disorders which can be further useful in the diagnosis and treatment of these disorders.

**Keywords**: Liver; reaction-diffusion equation; calcium; finite volume method; Newton-Raphson method

**AMS 2020 Classification**: 65N08; 92-10; 35-04; 92C37

## 1 Introduction

The largest organ in the body is the liver. The liver is located just above the stomach and below the diaphragm in the upper right abdomen. Liver weighs about 838 to 2584 grams, is reddish brown in colour and is slightly conical shaped. This organ is extra soft and fleshy. It is the only organ that can completely regenerate from a small part of itself [1, 2]. Liver cells are classified into

➤ **Received:** 30.01.2023 ➤ **Revised:** 15.03.2023 ➤ **Accepted:** 18.03.2023 ➤ **Published:** 31.03.2023

two categories viz Parenchymal cells and Non-Parenchymal cells. The Parenchymal cells of the liver are hepatocytes. Hepatocyte cells are cubical epithelial cells. This cell lines the sinusoids and makes up to 70% of cells in the liver. Cells within the liver that are not hepatocytes are collectively called as Non- Parenchymal cells. These cells serve a wide variety of metabolic, immune, and structural functions [3]. The Non-Parenchymal cells line up the normal liver sinusoid consisting of four different types of cells which are kuffer, endothelial/cholangiocyte, pit and stallete/ito cells. These cells differ in origin, population kinetics, phenotypic and functional characteristics [4]. A network of bile ducts or cholangiocytes lines the biliary tree. These are a diverse and highly active group of epithelial cells. Cholangiocytes collect bile from bile canaliculi from the hearing canals of hepatocytes. Primitive bile is generated in hepatocytes. Bile reaches to the gallbladder, choledochal, and extrahepatic duct using a network of channels. Only 3-5 percent of the overall number of liver cells are cholangiocyte cells [5]. The ability of a cell to accept, process, and disseminate signals to its surrounding and with itself is known as 'cellular communication' or 'signaling' [6]. $Ca^{2+}$ in the intracellular environment regulates a large number of functions like cell proliferation, apoptosis and secretion. The secretion of bile juice is one of the liver's most critical activities, it is the end consequence of hepatocytes producing bile whereas cholangiocytes condition it [6, 7]. When calcium is released from the endoplasmic reticulum (ER) through $IP_3$ receptors, inositol 1,4,5 triphosphate ($IP_3$) regulates calcium signaling in the cholangiocytes [8, 9]. Calcium signaling has been studied in various cells like neurons, oocytes, myocytes, astrocytes, pancreatic acinar cells, hepatocytes, etc. by various researchers [10–12, 15–25, 27]. Kotwani et al. constructed and simulated a one-dimensional unsteady state case mathematical model of calcium concentration in fibroblast cells using the finite difference approach [10]. Panday et al. constructed a model involving reaction-diffusion equations to study $Ca^{2+}$ distribution in oocyte cells involving $Na^+/Ca^{2+}$ exchanger and advection of calcium [11]. Naik et al. studied the calcium distribution involving voltage-gated calcium channels (VGCC), ryanodine receptors, and buffers in one, two and three dimensions for oocyte and T lymphocyte cells. They concluded that the increase of $Ca^{2+}$ concentration due to RYR was higher than that of VGCC [12–14, 60, 62]. Introducing a two-dimensional discrete-time chemical model and the existence of its fixed points, the one and two-parameter bifurcations of the model were also investigated by them [61]. Jha et al. studied calcium distribution using the finite element approach in astrocytes [15]. An attempt was also made by them to consider a one-dimensional fractional diffusion equation to study the effects of buffers and endoplasmic reticulum on the calcium distribution profile in nerve cells [63].
Amrita et al. observed the effects of $Na^+/Ca^{2+}$ exchanger, source geometry, leak, SERCA pump, etc. on $Ca^{2+}$ oscillations in dendritic spines & neuron cells employing finite element approach [16–18]. Pathak et al. devised a mathematical model for calcium distribution in cardiac myocytes involving a pump, excess buffer and leaks [19]. Manhas et al. observed calcium variation in pancreatic acinar cells describing the effect of mitochondria on $Ca^{2+}$ signaling [20–22]. Tewari et al. have constructed a model for neuron cells expressing the impact of sodium pump on $Ca^{2+}$ oscillation and calcium diffusion with excess buffer [23, 24]. Jagtap et al. solved interdependent calcium and $IP_3$ dynamics involving calcium flux, calcium diffusion coefficient, and protein content in the cytoplasm [25]. They also solved the problem for calcium concentration fluctuation in two dimensions using the finite volume method for the unsteady state situation [26]. Hemant et al. formulated an unsteady state mathematical model in one dimension to explore the distribution of intracellular calcium in T lymphocyte cells. The model takes into account factors including buffers, ryanodine receptors (RyRs), source influx and diffusion coefficient [27]. Kothiya et al. provided a mathematical model to analyze the $Ca^{2+}$ signaling to affect the synthesis of ATP and $IP_3$ in fibroblast cells [28, 29]. Bhardwaj et al. used a radial basis function-based differential quadrature method to examine the nonlinear spatiotemporal dynamics of $Ca^{2+}$ in T cells while accounting for

the SERCA pump, ryanodine receptor, source amplitude, and buffers [30]. Pawar et al. studied interdependent calcium and $IP_3$ dynamics and their effects on nitric oxide production and $\beta$-amyloid production and degradation in neuron cells. They also simulated the interdependent dynamics of calcium with dopamine, nitric oxide and $\beta$- amyloid in neuron cells [49–53]. Joshi et al. presented a calcium dynamics model that firmly orchestrates exchanges of calcium flux through intracellular/extracellular sources of calcium to investigate cellular activities and calcium homeostasis using a generalized two-dimensional space-time reaction-diffusion model [56].
Protein and voltage-dependent calcium channels were also used to obtain an approximate $Ca^{2+}$ profile by the fractional integral transform method [55]. A mathematical model of calcium was developed in the form of the Hilfer fractional reaction-diffusion equation to examine the calcium diffusion in the neuron cells. The effects of calcium-dependent protein and flux through the sodium-calcium exchanger were incorporated in the model [59]. Pankratova et al. employed bifurcation theory analysis and examined steady-state solutions, bistability, simple and complicated periodic limit cycles and also chaotic attractors for calcium variation in astrocytes [54]. Tarifa et al. demonstrated that preferential calcium release near the sarcolemma is key to a higher spatiotemporal distribution of sparks and amplitude of post-depolarizations in atrial myocytes from patients with atrial fibrillation using mathematical model [57]. Chang et al. developed a mathematical model of intracellular calcium dynamics for evaluating the combined anticancer effects of Afatinib and RP4010 in esophageal cancer [58].
Minagawa et al. have discussed that in almost every kind of cell, cytosolic $Ca^{2+}$ is an essential second messenger. Furthermore, $Ca^{2+}$ controls a variety of actions in individual cells. They looked at the cellular level machinery in cholangiocytes which is responsible for $Ca^{2+}$ signaling. Two $Ca^{2+}$ -mediated events have also been found in cholangiocytes which are apoptosis and bicarbonate secretion. They concluded that calcium signaling is responsible for therapeutically treating cholestatic disorders [31]. Nathanson et al. addressed the control of intracellular $Ca^{2+}$ channel expression in cholangiocytes [32]. Woo et al. formulated a model of the human biliary system and found that the release of ATP is closely co-related with shear which is dependent on intracellular $Ca^{2+}$ and becomes desensitized with repeated exposure to flow. Additionally, they found that activating membrane P2Y (Purinergic) receptors and ATP release both contribute to the increase in fluid flow's effect on $Ca^{2+}$ [33]. Weerachayaphorn et al. explained that cholangiocyte abnormalities are the primary cause of the majority of cholestatic diseases. The inositol 1,4,5-triphosphate receptor (IP3R), an intracellular calcium release channel, is most frequently seen in cholangiocytes as its type 3 isoform. In individuals with cholestatic diseases, IP3R expression is decreased in the intrahepatic bile ducts, which are necessary for the bile ducts to secrete bicarbonate. It was also examined how the oxidative stress-sensitive nuclear factor erythroid 2-like 2 (NFE2L2 or NRF2) controls the expression of IP3R [34]. Ueasilamongkol et al. examined cholangiocarcinoma (the second most common kind of liver cancer) using the type 3 variant of the inositol 1,4,5-triphosphate receptor [35]. Shibao et al. examined the effects of the inositol 1,4,5-triphosphate receptor (IP3R) ($Ca^{2+}$ release channel) in cholestasis-related animal models and patients on ductular secretion and $Ca^{2+}$ signaling [36]. Rodrigues et al. analyzed the mechanisms underlying $Ca^{2+}$ signals in cholangiocyte cells and used the experimental approaches to find cholangiocyte $Ca^{2+}$ signaling. The role of $Ca^{2+}$ in the regular and abnormal control of secretion and apoptosis in cholangiocytes was also explored [37]. Masyuk et al. explored the idea that the sensory organelles known as cholangiocyte cilia gather up and transmit information from luminal bile flow into intracellular $Ca^{2+}$ and adenosine $3^{'}$, $5^{'}$ cAMP (cyclic adenosine monophosphate) signaling [38]. Marzioni et al. examined to see if glucagon-like peptide-1 modifies the biological response of cholangiocytes to cholestasis [39]. Martin et al. suggested that the loss of IP3Rs may be the most widely used cause of cholestasis. It seems crucial for healthy bile secretion in the liver

that IP3R-mediated $Ca^{2+}$ signaling occurs in bile duct epithelia [40]. Maroni et al. determined that cholangiocytes react to injury by secreting a number of peptides, acquiring a neuroendocrine-like character. These substances alter cholangiocyte biology and control the progression of biliary injury through an autocrine/paracrine mechanism.
Cholangiopathies, a class of illnesses that targets biliary cells exclusively, are thought to progress more slowly as a result of the failure of such mechanisms [41]. Lazaridis et al. discussed the various diseases occurring in cholangiocytes such as inflammation, cholestasis, apoptotic death, and ductopenia, etc. due to dysregulation in calcium signaling [42]. Jung et al. explained the cAMP-induced processes in epithelial cells work in conjunction with calcium signaling to control membrane transport proteins and play a role in bicarbonate secretion [43]. Guerra et al. discussed the molecular processes that control cholangiocytes' bile production. Furthermore, there is evidence that certain cholestatic disorders of the bile ducts modify several aspects of the $Ca^{2+}$ signaling system, including the cholangiocytes's regulation of the expression of intracellular $Ca^{2+}$ channels [44]. Amaya et al. investigated the evidence indicating cholangiocyte $Ca^{2+}$ signaling defects are a major factor in the development of cholestatic diseases characterized by decreased hepatic bile secretion [45]. Shin et al. found that anion channels can equally fulfill a variety of physiological functions including regulation of neuronal excitability and secretion of epithelial fluid [46]. Alpini et al. suggested that a special absorption mechanism must exist in cholangiocytes for bile acid activity. Simultaneously cholangiocytes express a bile acid transporter [47]. A good number of investigations is reported on calcium distribution in various cells like neurons, oocytes, pancreatic acinar cells, hepatocytes, etc mostly using linear reaction-diffusion equations. Most of the investigations of calcium distribution in cells of the liver are reported for hepatocyte cells. But very little attention has been paid to understanding the calcium distribution patterns in cholangiocyte cells and that too is mostly experimental.
None of the theoretical studies on calcium distribution patterns in cholangiocyte cells have explored the role of buffers, SERCA pump, efflux, influxes, etc. Therefore the mechanisms of calcium signaling regulating the functions of cholangiocyte cells are not well understood to date. The insights of these mechanisms will be useful in understanding the processes leading to cholestasis diseases. In view of the above, the present study is focused on developing a mathematical model of calcium distribution in cholangiocyte cells. A nonlinear steady-state reaction-diffusion model of calcium ions in cholangiocyte cells is proposed by incorporating parameters like buffer, SERCA pump, influxes, efflux, etc. The numerical simulation is performed using the Finite Volume method and Newton Raphson method to analyze the effects of these parameters on calcium signaling in cholangiocyte cells.

## 2 Mathematical formulation of the problem

Mathematical modelling plays a key role in finding solutions to many real-world problems. The experimental approaches are very tedious and time-consuming therefore scientists prefer to make use of computational approaches for solving the problems. The computational approaches are congenial and hence adaptable. In the present study, the mathematical model and the solution of $Ca^{2+}$ signaling in cholangiocyte cell is presented.
The reaction-diffusion equation for $Ca^{2+}$ distribution in steady state for cholangiocyte is given by [48].

$$D_{Ca}\frac{\partial^2[Ca^{2+}]}{\partial x^2} + J_{IP3R} + J_{RYR} - J_{SERCA} + J_{IN} - J_{out} - k^+[B]_\infty([Ca^{2+}] - C_\infty) = 0. \tag{1}$$

$D_{Ca}$ represents diffusion coefficient, $k^+$ represents buffer association rate, $[B]_\infty$ represents buffer

concentration at equilibrium, $[Ca^{2+}]_\infty$ represents calcium concentration at equilibrium, $J_{IPR}$ represents influx from $IP_3$ receptor, $J_{RYR}$ represents influx from ryanodine receptor, $J_{SERCA}$ represents efflux into ER, $J_{IN}$ represent influx from plasma membrane, $J_{out}$ represent outflux from plasma membrane.
The fluxes are modelled as,

$$J_{IP3R} + J_{RYR} = k_1(T + T_0)(C_e - [Ca^{2+}]), \tag{2}$$

where $T$ indicates the basal fractional activity of the channels in the store, $T_0$ represents the calcium release rate from the store and $k_1$ denotes the rate of calcium release from the store.

$$J_{IN} = k_5(T + T_0)(C_{out} - [Ca^{2+}]), \tag{3}$$

$k_5$ represents external medium calcium influx and $C_{out}$ represents extracellular calcium concentration.

$$J_{out} = \frac{V_6[Ca^{2+}]^2}{k_7^2 + [Ca^{2+}]^2}, \tag{4}$$

The plasma membrane pump's maximal rate is represented by $V_6$ and its dissociation constant is represented by $k_7$.

$$J_{SERCA} = \frac{V_{serca}[Ca^{2+}]^2}{k_4^2 + [Ca^{2+}]^2}, \tag{5}$$

$V_{serca}$ represents the maximum rate of calcium pumping into the store and $k_4$ represents the storage calcium pump's dissociation constant.
Calcium concentration in ER can be replaced by,

$$C_e = \frac{(C_T - V_c)[Ca^{2+}]}{V_e}, \tag{6}$$

$C_T$ represents calcium concentration in cell and $C_e$ represent the calcium in ER.

Boundary condition: It is assumed that the influx source channel is present at $x = 0$. Therefore, the following flux condition is enforced:

$$lim_{x\to 0}\left(-D_{Ca}\left(\frac{\partial[Ca^{2+}]}{\partial x}\right)\right) = \sigma_{Ca}, \tag{7}$$

$\sigma_{Ca}$ represents source influx [25]. The other end of the cell $(x = 10)$ is assumed to be at rest. Therefore, a constant resting calcium concentration is assumed as given below:

$$lim_{x\to 10}([Ca^{2+}]) = C_\infty = 0.1\mu M, \tag{8}$$

**Solution:** The cytosol of the cholangiocyte cell is split into 20 nodes. By putting all the various

fluxes in Eq. (1), it can be rewritten as

$$D_{Ca}\frac{\partial^2[Ca^{2+}]}{\partial x^2} - k^+[B]_\infty([Ca^{2+}] - C_\infty) + k_1(T+T_0)\left(\frac{(C_T - V_c)[Ca^{2+}]}{V_e} - [Ca^{2+}]\right) + k_5(T+T_0)(C_{out} - [Ca^{2+}]) - \frac{V_{serca}[Ca^{2+}]^2}{k_4^2 + [Ca^{2+}]^2} - \frac{V_6[Ca^{2+}]^2}{k_7^2 + [Ca^{2+}]^2} = 0. \tag{9}$$

Representing calcium concentration in the cytosol of the cell ($[Ca^{2+}]$) by $u$, Eq. (9) can be written as,

$$D_{Ca}\frac{\partial^2 u}{\partial x^2} + k_1(T+T_0)(\frac{(C_T - V_c)u}{V_e} - u) + k_5(T+T_0)(C_{out} - u) - \frac{V_{serca}u^2}{k_4^2 + u^2} - \frac{V_6 u^2}{k_7^2 + u^2} - k^+[B]_\infty(u - C_\infty) = 0, \tag{10}$$

In general, Eq. (10) can be written as,

$$\frac{\partial^2 u}{\partial x^2} - au + c - \frac{V_{serca}u^2}{k_4^2 + u^2} - \frac{V_6 u^2}{k_7^2 + u^2} = 0, \tag{11}$$

$a$ and $c$ are given as,

$$a = \frac{k^+[B]_\infty + \frac{k_1(T+T_0)(V_c+V_e)}{V_e} + k_5(T+T_0)C_{out}}{D_{Ca}}, \tag{12}$$

$$c = \frac{k^+[B]_\infty C_\infty + \frac{k_1(T+T_0)C_T}{V_e} + k_5(T+T_0)}{D_{Ca}}. \tag{13}$$

To solve Eq. (11) finite volume method is employed. For the first term in Eq. (11), a linear profile assumption is taken for calcium concentration, and for the rest of the term, a constant profile assumption is taken. On integrating from $w$ to $e$ over control volumes,

$$\left(\frac{\partial u}{\partial x}\right)_e - \left(\frac{\partial u}{\partial x}\right)_w - au_G\delta x + c\delta x - \frac{V_{serca}u^2}{k_4^2 + u^2} - \frac{V_6 u^2}{k_7^2 + u^2} = 0, \tag{14}$$

where $u_G$ represents calcium concentration at the centroid point for any element.
For first control volume (n=1) Eq. (11) can be written as,

$$\left(\frac{\partial u}{\partial x}\right)_e + \frac{\sigma_{Ca}}{D_{Ca}} - au_G\delta x + c\delta x - \frac{V_{serca}u^2}{k_4^2 + u^2} - \frac{V_6 u^2}{k_7^2 + u^2} = 0. \tag{15}$$

Since linear profile assumption is taken for calcium concentration for the first term in Eq. (8), Eq. (12) can be rewritten as

$$\frac{u_E - u_G}{\delta x} + \frac{\sigma_{Ca}}{D_{Ca}} - au_G\delta x + c\delta x - \frac{V_{serca}u^2}{k_4^2 + u^2} - \frac{V_6 u^2}{k_7^2 + u^2} = 0. \tag{16}$$

After rearranging the terms,

$$\left(\frac{1}{\delta x}+a\delta x\right)u_G=\frac{1}{\delta x}u_E+\frac{\sigma_{Ca}}{D_{Ca}}+c\delta x-\frac{V_{serca}u^2}{k_4^2+u^2}-\frac{V_6u^2}{k_7^2+u^2}. \tag{17}$$

For last control volume (n=20), $u_E$ is 0.1 $\mu$M ($C_\infty$)

$$\frac{u_E-u_G}{\delta x}-\frac{u_G-u_w}{\delta x}-au_G\delta x+c\delta x-\frac{V_{serca}u^2}{k_4^2+u^2}-\frac{V_6u^2}{k_7^2+u^2}=0, \tag{18}$$

$$\left(\frac{2}{\delta x}+a\delta x\right)u_G=\frac{1}{\delta x}u_w+c\delta x+\frac{C_\infty}{\delta x}-\frac{V_{serca}u^2}{k_4^2+u^2}-\frac{V_6u^2}{k_7^2+u^2}. \tag{19}$$

For intermediate control volumes (n=2 to 19),

$$\frac{u_E-u_G}{\delta x}-\frac{u_G-u_w}{\delta x}-au_G\delta x+c\delta x-\frac{V_{serca}u^2}{k_4^2+u^2}-\frac{V_6u^2}{k_7^2+u^2}=0, \tag{20}$$

it is rewritten as,

$$\left(\frac{2}{\delta x}+a\delta x\right)u_G=\frac{1}{\delta x}u_E+\frac{1}{\delta x}u_w+c\delta x+\frac{C_\infty}{\delta x}-\frac{V_{serca}u^2}{k_4^2+u^2}-\frac{V_6u^2}{k_7^2+u^2}. \tag{21}$$

The resulting system of nonlinear equations is resolved using Newton Raphson's method.

## 3 Results and discussion

The following physiological parameters are used for solving the formulated problem in Eq. (11).

**Table 1.** Parameters of physiology affecting calcium variation [16, 26]

| Symbol | Parameter | Value |
|---|---|---|
| $D_{Ca}$ | Calcium's diffusion coefficient | 50 $\mu$ $m^2sec^{-1}$ |
| $k_1$ | Rate of calcium release from store | 7.5 $sec^{-1}$ |
| $K_2$ | Buffer association rate | 300 $\mu^{-1}M^{-1}sec^{-1}$ |
| $V_{serca}$ | Store pump dissociation constant | 0.65 $\mu Msec^{-1}$ |
| $k_4$ | The storage calcium pump's dissociation constant | 0.1 $\mu$M |
| $k_5$ | Calcium influx rate from the external medium | 0.000158 $sec^{-1}$ |
| $V_6$ | Plasma membrane pump's maximum rate | 2 µM/s $\mu Msec^{-1}$ |
| $k_7$ | Plasma membrane pump's dissociation constant | 0.6 $\mu$M |
| $C_{out}$ | Calcium concentration of extracellular medium | 2 $\mu$M |
| $T_0$ | The store's channel's baseline fractional activity | 0.2 |
| T | Activity on the store's channels in fractions | 0.8 |
| $C_T$ | Total $[Ca^{2+}]$ relative to cell volume | 2 $\mu$M |
| $k^+$ | Association rate of buffer | 1.5 $\mu M^{-1}sec^{-1}$ |
| $V_c$ | Volume of the cytosol to the total cell volume ratio | 0.83 |
| $V_e$ | Ratio of Volume of ER to total volume of cell | 0.3 |
| $C_\infty$ | Calcium concentration at Equilibrium | 0.1 $\mu$M |

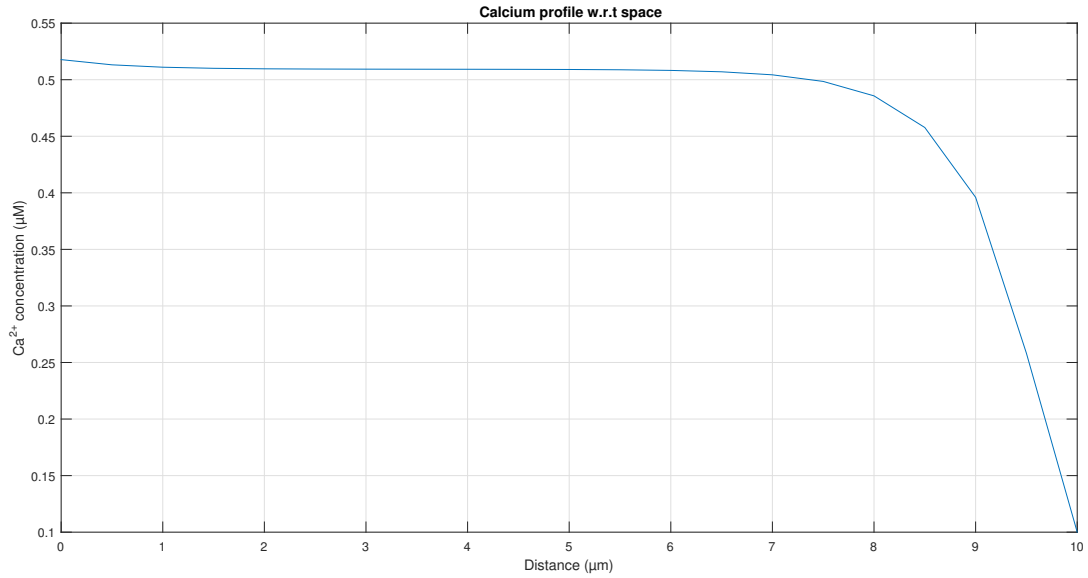


**Figure 1.** Calcium variation in cholangiocyte cell with respect to space

Figure 1 shows the calcium variation in a cholangiocyte cell with respect to space for diffusion coefficient 50 $\mu m^2 sec^{-1}$, source influx 1 pA and buffer 5 $\mu$M. By carefully studying the above graph, it shows that near the source, there was the highest concentration of calcium $\approx$ 0.53 $\mu$M. The calcium concentration continuously decreases until it reaches to its equilibrium value i.e. 0.1 $\mu$M, away from the source. The graph shows the non-linear behaviour of the calcium concentration pattern between $x$= 7 to 9 $\mu$m. This may be due to major imbalances among biophysical processes like diffusion, buffering, efflux, and influxes which is clear from the major difference in calcium concentration at $x$=7 $\mu$m and $x$=9 $\mu$m. The sharp fall from $x$=9 to $x$= 10 $\mu$m indicates the major role of buffering and calcium-reducing mechanisms in this area.

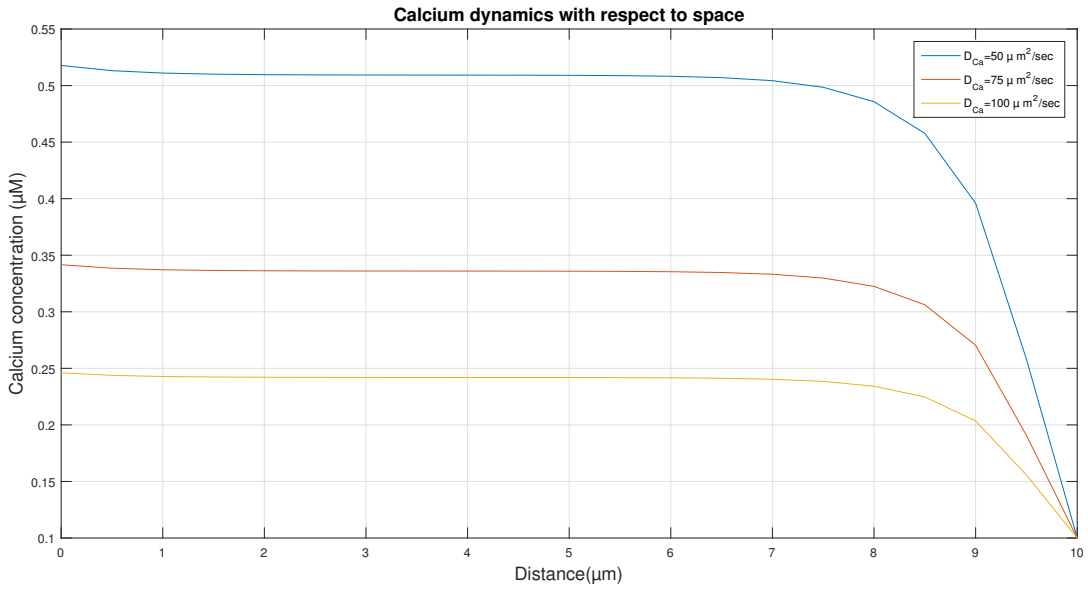


**Figure 2.** Cholangiocyte cell calcium change for various diffusion coefficient values with regard to space

Figure 2 shows the calcium variation with respect to space for source influx 1 pA, buffer 5 $\mu$M and diffusion coefficient 50 $\mu m^2 sec^{-1}$, 75 $\mu m^2 sec^{-1}$ and 100 $\mu m^2 sec^{-1}$. It can be observed from the figure that as the diffusion coefficient increases calcium concentration starts decreasing. This fall in calcium concentration with the increase in diffusion coefficient from $x = 0$ to $x = 9$ $\mu$m implies that the higher quantity of calcium is diffusing from the source towards the other end of the cell for higher rates of diffusion which further activates and increases the role of calcium reducing mechanisms like buffering etc. in the whole cell. The maximum value for calcium concentration is around 0.55 $\mu$M and the minimum value is 0.25 $\mu$M. Non-linear behaviour is the same as Figure 1. Moving away from the source calcium concentration starts decreasing gradually and it attains its equilibrium concentration 0.1 $\mu$M.

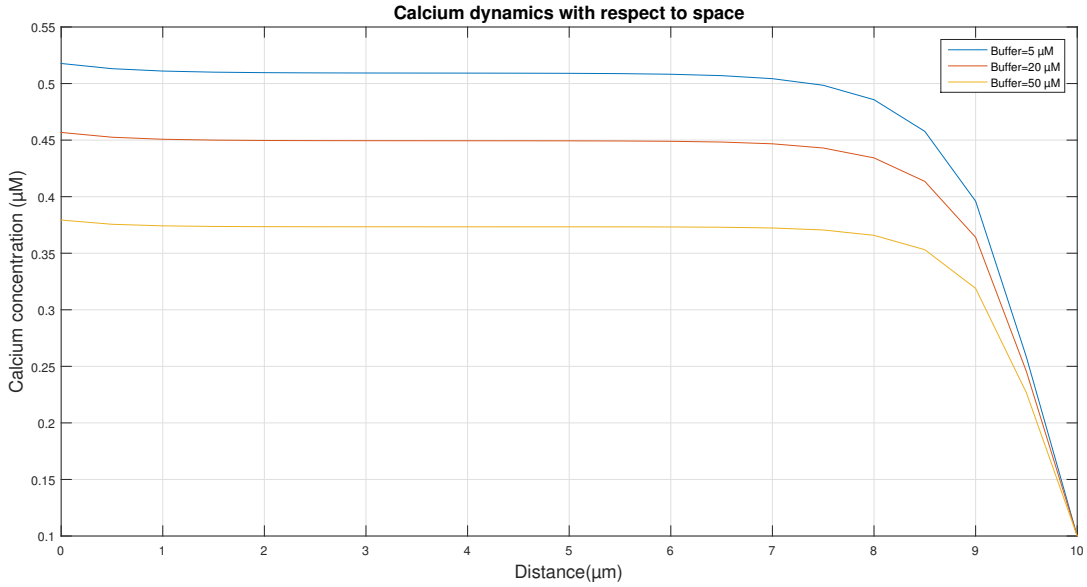


**Figure 3.** Calcium variation in cholangiocyte cell with respect to space for different value of buffer

Figure 3 shows the calcium concentration variation with respect to space for source influx 1 pA, buffer 5 $\mu$M, 20 $\mu$M and 50 $\mu$M and diffusion coefficient 50 $\mu m^2 sec^{-1}$. It can be observed from the figure as the buffer value increases calcium concentration starts decreasing. Free buffer binds with free calcium and forms calcium-bound buffer which decreases free calcium concentration. The maximum value for calcium concentration is around 0.55 $\mu$M and the minimum value is 0.38 $\mu$M. Non-linear behaviour is the same as Figure 1. Moving away from the source calcium concentration starts decreasing gradually and it attains its equilibrium concentration 0.1 $\mu$M.

Figure 4 shows the calcium variation with respect to space for source influx 1 pA , buffer 5 $\mu$M and diffusion coefficient 50 $\mu m^2 sec^{-1}$. A comparative study has been done for the rate of calcium influx from plasma membrane $k_1$ = 5.5 $sec^{-1}$, 7.5 $sec^{-1}$ and 15 $sec^{-1}$. It is evident from the graph that the concentration of calcium starts to increase as $k_1$ rises due to an increased influx of calcium from the plasma membrane. The maximum value for calcium concentration is around 0.95 $\mu$M and the minimum value is 0.38 $\mu$M. Non-linear behaviour is the same as Figure 1. Moving away from the source calcium concentration starts decreasing gradually and it attains its equilibrium concentration 0.1 $\mu$M.

Figure 5 shows the calcium concentration variation with respect to space for source influx 1 pA, buffer 5 $\mu$M and diffusion coefficient 50 $\mu m^2 sec^{-1}$. A comparative study has been done for the rate of calcium efflux to SERCA pump $V_{serca}$ 0.5 $\mu Msec^{-1}$, 0.65 $\mu Msec^{-1}$ and 1 $\mu Msec^{-1}$. It is evident

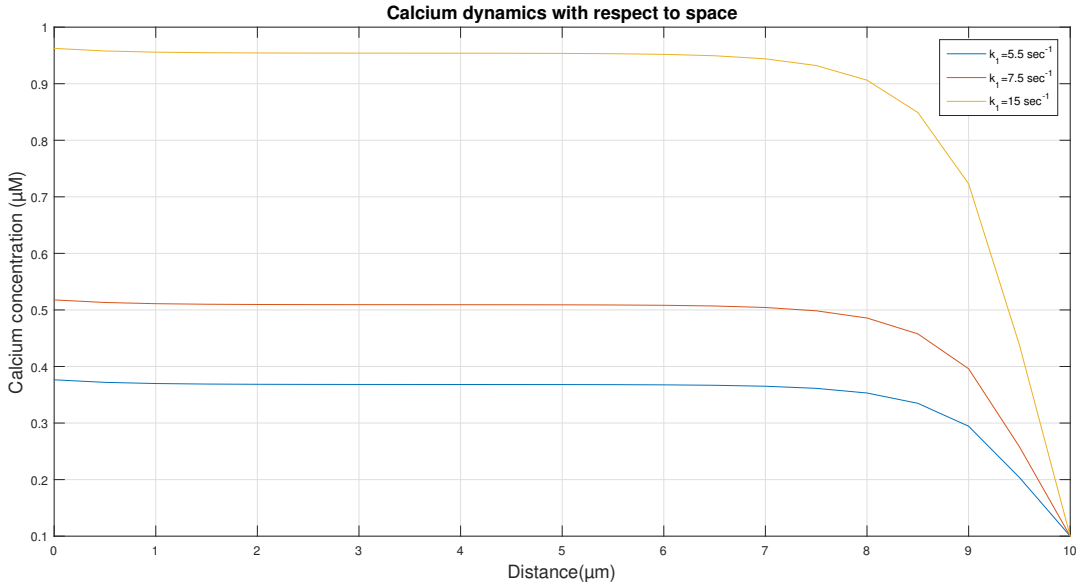


**Figure 4.** Calcium variation in cholangiocyte cell with respect to space for different value of $k_1$

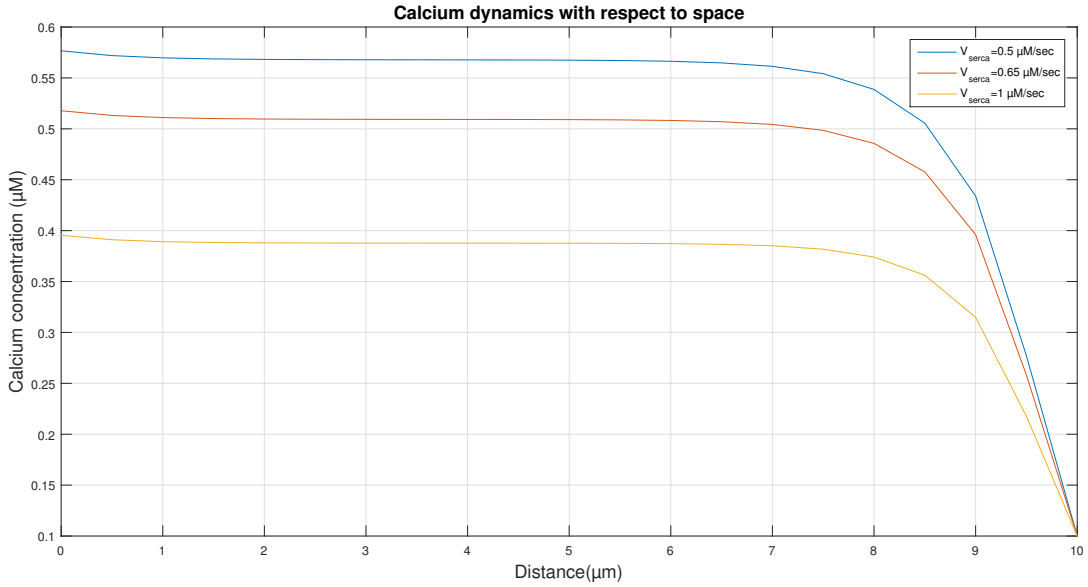


**Figure 5.** Calcium variation in cholangiocyte cell with respect to space for different values of $V_{serca}$

from the graph that the concentration of calcium starts to decrease as $V_{serca}$ rises due to SERCA pump which takes calcium out of the cytosol. The maximum value for calcium concentration is around 0.58 $\mu$M and the minimum value is 0.4 $\mu$M. Non-linear behaviour is the same as Figure 1. Moving away from the source calcium concentration starts decreasing gradually and it attains its equilibrium concentration 0.1 $\mu$M.

## 4 Conclusion

A reaction-diffusion model of calcium distribution patterns in cholangiocyte cells in constructed for a one-dimensional steady-state case and successfully simulated to analyze the impacts of various parameters incorporated in the model. The finite volume method can be used on arbitrary geometries, using structured or unstructured meshes and it leads to robust schemes. It

is locally conservative because it is based on 'balance' approach. The combination of the finite volume method and Newton's method has been successfully employed for solving the non-linear reaction-diffusion of calcium in the cell. The proposed numerical strategy for the simulation of the proposed nonlinear model provides novel insights into calcium distribution patterns in cholangiocyte cells. The following novel conclusions have been made on the basis of numerical results:

1. The calcium concentration variation shows nonlinear behaviour mostly near the boundary the cell maintained at resting calcium concentration along space. Most of the parts of cells are dominated by the effect of source influx. This is necessary due to the requirement of a high concentration of calcium for initiation, sustenance, and termination of the activity of the cell. The nonlinear behaviour observed in the region near the resting condition of calcium at the boundary is due to the role of calcium-reducing mechanisms like buffering and various efflux like SERCA pump.
2. The combined effect of calcium-reducing mechanisms like buffering and efflux like SERCA pump play the role depending on the requirement of the cell which is visible from Figure 1 and 2. This role is limited to a small region in Figure 1 but this role is more and in the whole region of the cell in response to increasing in diffusion coefficient in Figure 2.
3. The buffers have a crucial role in reducing the calcium concentration in the cell when efflux like SERCA pump is fixed or constant or limited or absent.
4. The role of $V_{serca}$ is crucial in reducing the calcium concentration in the cell when buffer quantity is fixed or constant or limited or absent.
5. The relation between calcium concentration and diffusion coefficient is inversely proportional that is the calcium concentration decreases with an increase in the diffusion coefficient.
6. The rise in calcium concentration is directly proportional to the rate of calcium release by storing the plasma membrane.

These novel insights obtained from the proposed model can be useful in understanding the mechanisms of the cells during health and disease. The present study was focused on calcium signaling in normal cholangiocyte cells. This model can be extended to the cells involving cholangiocyte disorders leading to various diseases like biliary cirrhosis etc. The present study provides the base for the development of models to evaluate abnormalities in mechanisms that can cause cholestatic disorders. The fractional processes of diffusion and Brownian motion can be incorporated in the future to develop a model of calcium distribution in cholangiocyte cells under various conditions. Various numerical and mathematical approaches like finite element method, cubic spline and iterated functional spaces can be explored in the future under various conditions. In the future, calcium signaling can be combined with other signaling systems to develop a systems biology model for cholangiocyte cells.

## Declarations

### Consent for publication

Not applicable.

### Conflicts of interest

The authors declare that they have no conflict of interest.

## Funding

Not applicable.

## Author's contributions

N.: Conceptualization; V.M.: Conceptualization, Methodology, Writing - Original Draft, Graphics, Analysis, Investigation, Visualization, Software; N.A.: Review and editing of the manuscript. All authors discussed the results and contributed to the final manuscript.

## Acknowledgements

Not applicable.

## References

[1] Wake, K. Perisinusoidal stellate cells (fat-storing cells, interstitial cells, lipocytes), their related structure in and around the liver sinusoids, and vitamin A-storing cells in extrahepatic organs. *International review of cytology*, 66, 303-353, (1980). [CrossRef]

[2] Tabibian, J.H., Masyuk, A.I., Masyuk, T.V., O'Hara, S.P., & LaRusso, N.F. Physiology of cholangiocytes. *Comprehensive Physiology*, 3(1), (2013). [CrossRef]

[3] Wang, D.Q.H., Neuschwander-Tetri, B.A., & Portincasa, P. The Biliary System, Colloquium Series on Integrated Systems Physiology: From Molecule to Function. *Morgan & Claypool*, 109-145,(2012).

[4] Bouwens, L., De Bleser, P., Vanderkerken, K., Geerts, B., & Wisse, E. Liver cell heterogeneity: functions of non-parenchymal cells. *Enzyme*, 46, 155-168, (1992).

[5] Strazzabosco, M., & Fabris, L. Functional anatomy of normal bile ducts. *The Anatomical Record: Advances in Integrative Anatomy and Evolutionary Biology*, 291(6), 653-660, (2008). [CrossRef]

[6] Minagawa, N., Kruglov, E.A., Dranoff, J.A., Robert, M.E., Gores, G.J., & Nathanson, M.H. The anti-apoptotic protein Mcl-1 inhibits mitochondrial $Ca^{2+}$ signals. *Journal of Biological Chemistry*, 280(39), 33637-33644, (2005). [CrossRef]

[7] Fiorotto, R., Spirlì, C., Fabris, L., Cadamuro, M., Okolicsanyi, L., & Strazzabosco, M. Ursodeoxycholic acid stimulates cholangiocyte fluid secretion in mice via CFTR-dependent ATP secretion. *Gastroenterology*, 133(5), 1603-1613, (2007). [CrossRef]

[8] Li, Q., Dutta, A., Kresge, C., Bugde, A., & Feranchak, A.P. Bile acids stimulate cholangiocyte fluid secretion by activation of transmembrane member 16A $Cl^{-}$ channels. *Hepatology*, 68(1), 187-199, (2018). [CrossRef]

[9] Hirata, K., Dufour, J.F., Shibao, K., Knickelbein, R., O'Neill, A.F., Bode, H.P., ... & Nathanson, M.H. Regulation of $Ca^{2+}$ signaling in rat bile duct epithelia by inositol 1, 4, 5-trisphosphate receptor isoforms. *Hepatology*, 36(2), 284-296, (2002). [CrossRef]

[10] Kotwani, M., & Adlakha, N. Modeling of endoplasmic reticulum and plasma membrane $Ca^{2+}$ uptake and release fluxes with excess buffer approximation (EBA) in fibroblast cell. *International Journal of Computational Materials Science and Engineering*, 6(01), 1750004, (2017). [CrossRef]

[11] Panday, S., & Pardasani, K. R. Finite element model to study effect of advection diffusion and $Na^{+}/Ca^{2+}$ exchanger on $Ca^{2+}$ distribution in oocytes. *Journal of medical imaging and health informatics*, 3(3), 374-379, (2013). [CrossRef]

[12] Naik, P.A., & Pardasani, K.R. One dimensional finite element model to study calcium distri-

bution in oocytes in presence of VGCC, RyR and buffers. *Journal of Medical Imaging and Health Informatics*, 5(3), 471-476, (2015). [CrossRef]

[13] Naik, P.A., & Pardasani, K.R. Finite element model to study calcium distribution in oocytes involving voltage gated $Ca^{2+}$ channel, ryanodine receptor and buffers. *Alexandria Journal of Medicine*, 52(1), 43-49, (2016). [CrossRef]

[14] Naik, P.A., & Pardasani, K.R. Three-dimensional finite element model to study effect of RyR calcium channel, ER leak and SERCA pump on calcium distribution in oocyte cell. *International Journal of Computational Methods*, 16(01), 1850091, (2019). [CrossRef]

[15] Jha, B.K., Adlakha, N., & Mehta, M.N. Finite element model to study calcium diffusion in astrocytes. *Int. J. of Pure and Appl. Math*, 78(7), 945-955, (2012).

[16] Jha, A., & Adlakha, N. Finite element model to study the effect of exogenous buffer on calcium dynamics in dendritic spines. *International Journal of Modeling, Simulation, and Scientific Computing*, 5(02), 1350027, (2014). [CrossRef]

[17] Jha, A., Adlakha, N., & Jha, B.K. Finite element model to study effect of $Na^{+}$-$Ca^{2+}$ exchangers and source geometry on calcium dynamics in a neuron cell. *Journal of Mechanics in Medicine and Biology*, 16(02), 1650018, (2016). [CrossRef]

[18] Jha, A., & Adlakha, N. Two-dimensional finite element model to study unsteady state $Ca^{2+}$ diffusion in neuron involving ER LEAK and SERCA. *International Journal of Biomathematics*, 8(01), 1550002, (2015). [CrossRef]

[19] Pathak, K.B., & Adlakha, N. Finite element model to study calcium signalling in cardiac myocytes involving pump, leak and excess buffer. *Journal of Medical Imaging and Health Informatics*, 5(4), 683-688, (2015). [CrossRef]

[20] Manhas, N., & Anbazhagan, N. A mathematical model of intricate calcium dynamics and modulation of calcium signalling by mitochondria in pancreatic acinar cells. *Chaos, Solitons & Fractals*, 145, 110741, (2021). [CrossRef]

[21] Manhas, N., & Pardasani, K.R. Mathematical model to study $IP_3$ dynamics dependent calcium oscillations in pancreatic acinar cells. *Journal of Medical Imaging and Health Informatics*, 4(6), 874-880, (2014). [CrossRef]

[22] Manhas, N., & Pardasani, K.R. Modelling mechanism of calcium oscillations in pancreatic acinar cells. *Journal of bioenergetics and biomembranes*, 46, 403-420, (2014). [CrossRef]

[23] Tewari, S.G., & Pardasani, K.R. Modeling effect of sodium pump on calcium oscillations in neuron cells. *Journal of Multiscale Modelling*, 4(03), 1250010, (2012). [CrossRef]

[24] Tewari, S., & Pardasani, K.R. Finite element model to study two dimensional unsteady state cytosolic calcium diffusion in presence of excess buffers. *IAENG International Journal of Applied Mathematics*, 40(3), 108-112, (2010).

[25] Jagtap, Y., & Adlakha, N. Numerical study of one-dimensional buffered advection–diffusion of calcium and $IP_3$ in a hepatocyte cell. *Network Modeling Analysis in Health Informatics and Bioinformatics*, 8(1), 25, (2019). [CrossRef]

[26] Jagtap, Y., & Adlakha, N. Finite volume simulation of two dimensional calcium dynamics in a hepatocyte cell involving buffers and fluxes. *Communications in Mathematical Biology and Neuroscience*, 2018, 15, (2018).

[27] Kumar, H., Naik, P.A., & Pardasani, K.R. Finite element model to study calcium distribution in T lymphocyte involving buffers and ryanodine receptors. *Proceedings of the National Academy of Sciences, India Section A: Physical Sciences*, 88, 585-590, (2018). [CrossRef]

[28] Kothiya, A., & Adlakha, N. Model of Calcium Dynamics Regulating $IP_3$ and ATP Production in a Fibroblast Cell. *Advances in Systems Science and Applications*, 22(3), 49-69, (2022).

[29] Kothiya, A.B., & Adlakha, N. Cellular nitric oxide synthesis is affected by disorders in the interdependent $Ca^{2+}$ and $IP_3$ dynamics during cystic fibrosis disease. *Journal of Biological Physics*, 1-26, (2023). [CrossRef]

[30] Bhardwaj, H., & Adlakha, N. Radial Basis Function Based Differential Quadrature Approach to Study Reaction Diffusion of $Ca^{2+}$ in T Lymphocyte. *International Journal of Computational Methods*, (2022). [CrossRef]

[31] Minagawa, N., Nagata, J., Shibao, K., Masyuk, A.I., Gomes, D.A., Rodrigues, M.A., ... & Nathanson, M.H. Cyclic AMP regulates bicarbonate secretion in cholangiocytes through release of ATP into bile. *Gastroenterology*, 133(5), 1592-1602, (2007). [CrossRef]

[32] Nathanson, M.H., Burgstahler, A.D., Mennone, A.L.B.E.R.T., & Boyer, J.L. Characterization of cytosolic $Ca^{2+}$ signaling in rat bile duct epithelia. *American Journal of Physiology-Gastrointestinal and Liver Physiology*, 271(1), G86-G96, (1996). [CrossRef]

[33] Woo, K., Dutta, A.K., Patel, V., Kresge, C., & Feranchak, A.P. Fluid flow induces mechanosensitive ATP release, calcium signalling and $Cl^-$ transport in biliary epithelial cells through a PKC$\gamma$-dependent pathway. *The Journal of physiology*, 586(11), 2779-2798, (2008). [CrossRef]

[34] Weerachayaphorn, J., Amaya, M.J., Spirli, C., Chansela, P., Mitchell-Richards, K.A., Ananthanarayanan, M., & Nathanson, M.H. Nuclear factor, erythroid 2-like 2 regulates expression of type 3 inositol 1, 4, 5-trisphosphate receptor and calcium signaling in cholangiocytes. *Gastroenterology*, 149(1), 211-222, (2015). [CrossRef]

[35] Ueasilamongkol, P., Khamphaya, T., Guerra, M. T., Rodrigues, M.A., Gomes, D.A., Kong, Y., ... & Weerachayaphorn, J. Type 3 inositol 1, 4, 5-trisphosphate receptor is increased and enhances malignant properties in cholangiocarcinoma. *Hepatology*, 71(2), 583-599, (2020). [CrossRef]

[36] Shibao, K., Hirata, K., Robert, M.E., & Nathanson, M.H. Loss of inositol 1, 4, 5-trisphosphate receptors from bile duct epithelia is a common event in cholestasis. *Gastroenterology*, 125(4), 1175-1187, (2003). [CrossRef]

[37] Rodrigues, M.A., Gomes, D.A., & Nathanson, M.H. Calcium signaling in cholangiocytes: methods, mechanisms, and effects. *International Journal of Molecular Sciences*, 19(12), 3913, (2018). [CrossRef]

[38] Masyuk, A.I., Masyuk, T.V., Splinter, P.L., Huang, B.Q., Stroope, A.J., & LaRusso, N.F. Cholangiocyte cilia detect changes in luminal fluid flow and transmit them into intracellular $Ca^{2+}$ and cAMP signaling. *Gastroenterology*, 131(3), 911-920, (2006). [CrossRef]

[39] Marzioni, M., Alpini, G., Saccomanno, S., Candelaresi, C., Venter, J., Rychlicki, C., ... & Benedetti, A. Glucagon-like peptide-1 and its receptor agonist exendin-4 modulate cholangiocyte adaptive response to cholestasis. *Gastroenterology*, 133(1), 244-255, (2007). [CrossRef]

[40] Martin, J., & Dufour, J.F. Cholestasis shuts down calcium signaling in cholangiocytes. *Hepatology*, 39(1), 248-249, (2004). [CrossRef]

[41] Maroni, L., Haibo, B., Ray, D., Zhou, T., Wan, Y., Meng, F., ... & Alpini, G. Functional and structural features of cholangiocytes in health and disease. *Cellular and molecular gastroenterology and hepatology*, 1(4), 368-380, (2015). [CrossRef]

[42] Lazaridis, K.N., Strazzabosco, M., & LaRusso, N.F. The cholangiopathies: disorders of biliary epithelia. *Gastroenterology*, 127(5), 1565-1577, (2004). [CrossRef]

[43] Jung, J., & Lee, M.G. Role of calcium signaling in epithelial bicarbonate secretion. *Cell Calcium*,

55(6), 376-384, (2014). [CrossRef]

[44] Guerra, M.T., & Nathanson, M.H. Calcium signaling and secretion in cholangiocytes. Pancreatology, 15(4), S44-S48, (2015). [CrossRef]

[45] Amaya, M.J., & Nathanson, M.H. Calcium signaling and the secretory activity of bile duct epithelia. *Cell Calcium*, 55(6), 317-324, (2014). [CrossRef]

[46] Shin, D.H., Kim, M., Kim, Y., Jun, I., Jung, J., Nam, J.H., ... & Lee, M.G. Bicarbonate permeation through anion channels: its role in health and disease. *Pflügers Archiv-European Journal of Physiology*, 472, 1003-1018, (2020). [CrossRef]

[47] Alpini, G., Glaser, S.S., Rodgers, R., Phinizy, J.L., Robertson, W.E., Lasater, J., ... & LeSage, G.D. Functional expression of the apical Na+-dependent bile acid transporter in large but not small rat cholangiocytes. *Gastroenterology*, 113(5), 1734-1740, (1997). [CrossRef]

[48] Lopez-Caamal, F., Oyarzún, D.A., Middleton, R. H., & García, M.R. Spatial Quantification of Cytosolic $Ca^{2+}$ Accumulation in Non excitable Cells: An Analytical Study. *IEEE/ACM Transactions on Computational Biology and Bioinformatics*, 11(3), 592-603, (2014). [CrossRef]

[49] Pawar, A., & Pardasani, K.R. Effect of disturbances in neuronal calcium and $IP_3$ dynamics on $\beta$-amyloid production and degradation. *Cognitive Neurodynamics*, 1-18, (2022). [CrossRef]

[50] Pawar, A., & Pardasani, K.R. Simulation of disturbances in interdependent calcium and $\beta$-amyloid dynamics in the nerve cell. *The European Physical Journal Plus*, 137(8), 1-23, (2022). [CrossRef]

[51] Pawar, A., & Pardasani, K.R. Study of disorders in regulatory spatiotemporal neurodynamics of calcium and nitric oxide. *Cognitive Neurodynamics*, 1-22, (2022). [CrossRef]

[52] Pawar, A., & Pardasani, K.R. Computational model of calcium dynamics-dependent dopamine regulation and dysregulation in a dopaminergic neuron cell. *The European Physical Journal Plus*, 138(1), 30, (2023). [CrossRef]

[53] Pawar, A., & Raj Pardasani, K. Effects of disorders in interdependent calcium and $IP_3$ dynamics on nitric oxide production in a neuron cell. *The European Physical Journal Plus*, 137(5), 1-19, (2022). [CrossRef]

[54] Pankratova, E.V., Sinitsina, M.S., Gordleeva, S., & Kazantsev, V.B. Bistability and Chaos Emergence in Spontaneous Dynamics of Astrocytic Calcium Concentration. *Mathematics*, 10(8), 1337, (2022). [CrossRef]

[55] Joshi, H., & Jha, B.K. 2D dynamic analysis of the disturbances in the calcium neuronal model and its implications in neurodegenerative disease. *Cognitive Neurodynamics*, 1-12, (2022). [CrossRef]

[56] Joshi, H., & Jha, B.K. 2D memory-based mathematical analysis for the combined impact of calcium influx and efflux on nerve cells. *Computers & Mathematics with Applications*, 134, 33-44, (2023). [CrossRef]

[57] Tarifa, C., Vallmitjana, A., Jiménez-Sábado, V., Marchena, M., Llach, A., Herraiz-Martínez, A., ... & Hove-Madsen, L. *Spatial distribution of calcium sparks determines their ability to induce afterdepolarizations in human atrial myocytes. Basic to Translational Science*, 8(1), 1-15, (2023). [CrossRef]

[58] Chang, Y., Funk, M., Roy, S., Stephenson, E., Choi, S., Kojouharov, H. V., ... & Pan, Z. Developing a mathematical model of intracellular calcium dynamics for evaluating combined anticancer effects of afatinib and RP4010 in esophageal cancer. International Journal of Molecular Sciences, 23(3), 1763, (2022). [CrossRef]

[59] Joshi, H., & Jha, B.K. Chaos of calcium diffusion in Parkinson's infectious disease model and treatment mechanism via Hilfer fractional derivative. *Mathematical Modelling and Numerical Simulation with Applications*, 1(2), 84-94, (2021). [CrossRef]

[60] Naik, P.A. Modeling the mechanics of calcium regulation in T lymphocyte: a finite element method approach. *International Journal of Biomathematics*, 13(05), 2050038, (2020). [CrossRef]

[61] Naik, P.A., Eskandari, Z., & Shahraki, H.E. Flip and generalized flip bifurcations of a two-dimensional discrete-time chemical model. *Mathematical Modelling and Numerical Simulation with Applications*, 1(2), 95-101, (2021). [CrossRef]

[62] Naik, P.A., & Pardasani, K.R. Two dimensional finite element model to study calcium distribution in oocytes. *Journal of Multiscale Modelling*, 6(01), 1450002, (2015). [CrossRef]

[63] Jha, B.K., & Joshi, H. A Fractional Mathematical Model to Study the Effect of Buffer and Endoplasmic Reticulum on Cytosolic Calcium Concentration in Nerve Cells. *In Fractional Calculus in Medical and Health Science* (pp. 211-227), CRC Press, (2020). [CrossRef]

Mathematical Modelling and Numerical Simulation with Applications (MMNSA)
(https://dergipark.org.tr/en/pub/mmnsa)



**How to cite this article:** Nakul, N., Mishra, V. & Adlakha, N. (2023). Finite volume simulation of calcium distribution in a cholangiocyte cell. *Mathematical Modelling and Numerical Simulation with Applications*, 3(1), 17-32. https://doi.org/10.53391/mmnsa.1273945